

## Hydrogen Bonding in Polymer Blends. 4. Blends Involving Polymers Containing Methacrylic Acid and Vinylpyridine Groups

Joon Y. Lee, Paul C. Painter, and Michael M. Coleman\*

Department of Materials Science and Engineering, The Pennsylvania State University, University Park, Pennsylvania 16802. Received July 8, 1987

**ABSTRACT:** The results of a Fourier transform infrared study of poly(ethylene-co-methacrylic acid) (EMAA) copolymer blends with poly(2-vinylpyridine) (P2VP) and a copolymer of styrene and 2-vinylpyridine are presented. EMAA copolymers are strongly self-associated at ambient temperatures through the formation of intermolecular carboxylic acid dimers. P2VP, a polymer that is inherently weakly self-associated, forms a strong association with EMAA by forming intermolecular hydrogen bonds between the carboxylic acid and pyridine groups. The fraction of interacting sites in these blends plays a major role in determining the solution and film forming properties of the mixtures and ultimately the degree of molecular mixing of the two polymers. Quantitative measurements of the fraction of pyridine groups that are hydrogen bonded to carboxylic acid groups have been obtained, and the results are discussed in terms of competing equilibria.

In the previous papers of this series we have described FTIR studies of miscible blends of a polyurethane with poly(ethylene oxide-co-propylene oxide) (EPO)<sup>1,2</sup> and poly(ethylene-co-methacrylic acid) (EMAA) blends containing the polyethers poly(vinyl methyl ether) (PVME) and EPO<sup>3</sup>. Pure EMAA copolymers are strongly self-associated in the condensed state at ambient temperatures through the formation of intermolecular carboxylic acid dimers. Molecular mixing of EMAA, which requires the disassociation of some or most of these carboxylic acid dimers, is possible with chemically dissimilar polymers that are inherently weakly self-associated but contain specific sites that can potentially form favorable intermolecular interactions (notably hydrogen bonds) with EMAA. This may be described quantitatively in terms of competing equilibria.<sup>1-3</sup> Equilibrium constants,  $K_A$  and  $K_B$ , were employed to express the self-association of EMAA and the association of EMAA with PVME (or EPO), respectively, as depicted below.

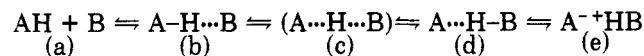


As we have demonstrated,<sup>3</sup> miscible systems are feasible even if the magnitude of  $K_B$  is much smaller than  $K_A$ . For the EMAA-polyether blends studied,  $K_A$  was determined to be approximately 2-3 orders of magnitude greater than  $K_B$ . It should be emphasized, however, that the relative strengths ( $\Delta H$ ) of the specific hydrogen bonded interactions associated with the carboxylic acid dimer and the carboxylic acid-ether pair are very similar. In marked contrast, the results presented in this paper are of a study of EMAA mixtures with polymers where the strength of the interaction AB is significantly greater than that of AA (self-association). Poly(2-vinylpyridine) (P2VP) and poly(2-vinylpyridine-co-styrene) (SP2VP) are two such polymers; they are inherently weakly self-associated but contain a basic nitrogen atom that can form a strong hydrogen bond with the carboxylic acid proton. As we will see, this leads to some unusual spectral features. Accordingly, we believe it useful to briefly review some of the fundamentals of hydrogen bonding before presenting our results.

There is a wealth of literature concerning hydrogen bonds in all their manifestations, summarized in various major reviews and books.<sup>4-9</sup> This work principally concerns small molecules, however, and *synthetic* polymers are largely ignored. It is clear from a review of this literature, however, that most workers are aiming at a fundamental understanding of the nature of the hydrogen bond. We are not. Rather, we wish to know what the existence of such bonds does to the properties of polymers and their mixtures.

Most of us are familiar with the type of hydrogen bonds that occur in synthetic polymers such as polyamides and polyurethanes.<sup>10-13</sup> The N-H stretching band shifts to lower frequency (compared to the "free" N-H stretching band), broadens significantly, and increases dramatically in intensity. Conceptually, the interpretation of the broad band in terms of a dynamic distribution of various structures containing different hydrogen bond strengths, which are intensity enhanced by changes in electronic structure, is intuitively pleasing to a polymer scientist.<sup>10</sup> In addition, there is a nice analogy to the statistics of linear polycondensation when one considers a description of the "chains" of hydrogen-bonding amide or urethane groups that are formed in terms of association models.<sup>1,13</sup> Things become more complex and the spectra more difficult to interpret as we consider progressively stronger hydrogen bonds. The spectroscopic characteristics of various hydrogen bonds have been nicely summarized by Hadzi,<sup>14,15</sup> Odínokov et al.,<sup>16</sup> and, in the special case of acid salts, Speakman.<sup>17</sup> Essentially, spectral features characteristic of three different categories of hydrogen bonds are identified: weak, medium, and strong (naturally, these categories are not exclusive and there exist intermediate "shades of gray").

One classification that ultimately depends upon the A...B interatomic distance is based on the different potential curves corresponding to the various species depicted in the following equilibrium scheme.



The classic Morse potential (or the semiempirical Schroeder-Lippincott function<sup>18,19</sup>) has been used to describe a lone or "free" A-H group to a first approximation (depicted as (a) above). For *weak* or *moderately strong* hydrogen bonds the hydrogen atom is located closer to one atom or the other (depicted as (b) and (d) above). The potential energy is correspondingly unsymmetric with a double minimum potential. The lower of the two minima is located near the donor atom. As the strength of the hydrogen bond increases and the A...B length decreases, the hydrogen atom is not so clearly identified as more strongly associated with one atom or the other (depicted as (c) above). Thus for *strong* hydrogen bonds we might expect a potential energy diagram with two equal (or nearly equal) potential minima having a low potential barrier between the two or, alternatively, a single symmetric potential energy curve with a truly broad minimum.

Having set the stage by setting up some (more or less) arbitrary criteria that allow us to place various hydrogen-bonded systems into certain categories, let us now consider the spectroscopic characteristics of each. It should

be kept in mind that this picture is necessarily painted with a broad brush and certain systems exhibit intermediate behavior. Additionally, we will not dwell upon the special characteristics of *weak* hydrogen bonds as we are familiar with the broad, usually structureless band profiles<sup>10,13</sup> centered near  $3300\text{ cm}^{-1}$ . As we progress to hydrogen bonds of *intermediate* strength, as in carboxylic acid dimers<sup>1</sup> or phenol-pyridine complexes (see ref 20 for the analogous polymer complex), the A-H stretching mode shifts to  $3100\text{--}2800\text{ cm}^{-1}$  and we start to observe so-called "satellite" bands superimposed upon the broad fundamental profile. These satellite bands are thought to arise from either overtones and combinations that are intensity enhanced by Fermi resonance or anharmonic coupling of the  $\nu_s$  (A-H stretching) and  $\sigma_g$  (H...B stretching) modes.<sup>21</sup>

As we move from intermediate to *strong* hydrogen bonds, the infrared spectra start to look very strange. In the paper of Odinokov et al. there are beautiful examples (see figures 1 and 2 in ref 16) of spectra for acid-base complexes corresponding to the series (b), (c), and (d) of the equilibrium scheme given above. For type I complexes (A-H...B), where the proton is not transferred, with increasing hydrogen bond strength, the A-H band "splits" into three characteristic intense broad bands (usually denoted A, B, and C) at about  $2800$ ,  $2500$ , and  $1800\text{ cm}^{-1}$ . As the proton becomes increasingly delocalized, or symmetrically placed between the A and B atoms, then broad bands (D and E) at about  $1200$  and  $700\text{ cm}^{-1}$  dominate the spectrum. Finally, at higher base strengths the situation reverses itself as the proton is now closer to the B atom (structure (d) in the equilibrium scheme above). A, B, and C bands between  $1800$  and  $3000\text{ cm}^{-1}$  return.

In this paper we will see some of the features attributed to strong hydrogen bonding in the infrared spectra of polymer blends containing methacrylic acid and pyridine groups. In addition, we will see how composition, defined in terms of the fraction of interacting sites, has a dramatic effect on the solution and film-forming properties of these blends.

### Experimental Section

The ethylenemethacrylic acid copolymers (EMAA) containing 18, 32, 44, and 55 wt % MAA (denoted EMAA[18], EMAA[32], etc.) were synthesized in the laboratories of the E.I. Du Pont de Nemours Co. and are described in the previous paper of this series.<sup>3</sup> A copolymer of 2-vinylpyridine and styrene (SP2VP[70]) containing 70 wt % of vinylpyridine was obtained from Polysciences Inc. Poly(2-vinylpyridine) (P2VP) was obtained from Reilly Tar and Chemical Corp. The latter two polymers are amorphous with  $T_g$ s of 99 and  $77\text{ }^\circ\text{C}$ , respectively.

Infrared spectra were recorded on either a Digilab Model FTS-15E or a FTS-60 Fourier transform infrared (FTIR) spectrometer at a resolution of  $2\text{ cm}^{-1}$ . A minimum of 64 scans were signal averaged, and the spectra were stored on a magnetic disc system. Spectra recorded at elevated temperatures were obtained by using a SPECAC high-temperature cell mounted in the spectrometer and a Micristar heat controller. This device has a reported accuracy of  $\pm 0.1\text{ }^\circ\text{C}$ . Diffuse reflectance infrared Fourier transform (DRIFT) spectra were obtained by using a COLLECTOR diffuse reflectance cell (Barnes/Spectra-Tech Inc.) and are presented in the Kubelka-Munk format.<sup>22</sup> Details of the preparation of samples for FTIR analysis are given in the text. Thermal analysis was performed on a Perkin-Elmer 7 Series differential scanning calorimeter. A heating rate of  $20\text{ }^\circ\text{C}/\text{min}$  was employed by using a sample size of approximately 10–15 mg.

### Results and Discussion

A summary of the major temperature dependent infrared spectral features attributed to the methacrylic acid structural unit has been presented in the previous paper of this series.<sup>3</sup> We have also previously reported on the

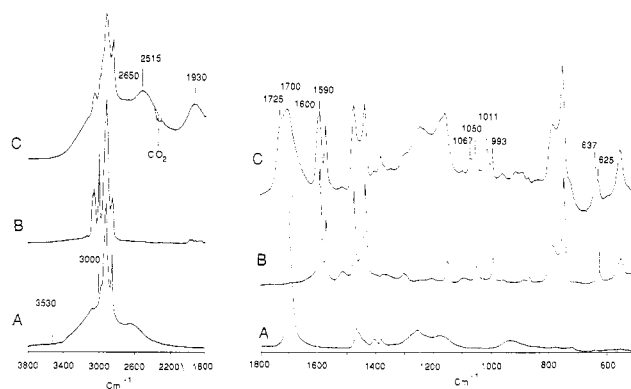


**Figure 1.** (A) Transmission infrared spectrum of a film of EMAA[55]. (B) DRIFT spectrum of a powdered sample of P2VP. (C) DRIFT spectrum of the EMAA[55]-P2VP powdered precipitate.

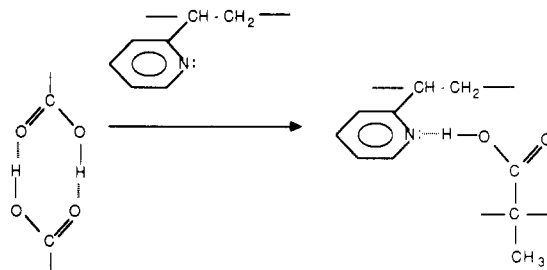


**Figure 2.** Schematic diagram illustrating the carboxylic acid-pyridine nitrogen interaction.

application of diffuse reflectance infrared Fourier transform (DRIFT) spectroscopy to powder samples of polymer complexes formed by precipitation from solution of poly(4-vinylphenol) (PVPh) and poly(2-vinylpyridine) (P2VP) in a common solvent.<sup>20</sup> The composition of this precipitated complex was found to be essentially independent of the composition of the initial ingredients. If we now repeat the experiment, but use EMAA[55] instead of PVPh, the result is the same; a precipitate is formed when dilute THF solutions of the two pure polymers are mixed. Scale expanded DRIFT spectra of the EMAA-P2VP complex together with the spectra of the pure components are shown in Figure 1. A purely schematic chemical representation of the complex given in Figure 2.

The EMAA[55] spectrum (denoted A) is dominated by the characteristic bands of self-association attributed to the intermolecular carboxylic acid dimer at about  $3000\text{ cm}^{-1}$  ( $\nu_s(\text{O-H})$ ),  $2650$  ("satellite" bands), and  $1700\text{ cm}^{-1}$  ( $\nu_s(\text{C=O})$ ). The most striking feature of Figure 1, however, is the presence of two broad bands in the top spectrum of the complex at  $2515$  and  $1930\text{ cm}^{-1}$ . These correspond to the "B" and "C" bands discussed above which are indicative of strong hydrogen bonds. It is of interest to note that these bands were not seen in the PVPh-P2VP complex;<sup>20</sup> the hydrogen bond formed in this case is significantly weaker with the  $\nu_s(\text{O-H})$  stretching frequency occurring beneath the CH stretching modes. The new band at about  $1725\text{ cm}^{-1}$ , which will be featured prominently in our forthcoming discussions, is indicative of a carbonyl group that is neither associated with an acid monomer or acid dimer but has been "liberated" as a consequence of the association of the acid hydroxyl group with the pyridine nitrogen atom in the formation of the complex (see Figure 2). Other spectral features of interest, which are potentially useful to our blend studies, concern the characteristic modes of the pyridine group at  $1590$ ,  $1050$ ,  $993$ , and  $625\text{ cm}^{-1}$ . Upon formation of the complex, these modes are perturbed and shift to  $1600$ ,  $1067$ ,  $1011$ , and  $634\text{ cm}^{-1}$ ,

Table I

EMAA/ P2VP	composition				
	20/80	35/65	50/50	65/35	80/20
EMAA[18]	clear solution throughout all compositions				
EMAA[32]	← precipitate →		← clear solution →		
EMAA[44]	precipitate throughout all compositions				
EMAA[55]					

respectively.<sup>23</sup> Again, an indication of the strength of the hydrogen bond formed between EMAA[55] and P2VP.

The precipitated EMAA[55]-P2VP complex is insoluble and cannot be fused together to form a coherent film without degrading the sample. One question that comes to mind is, "if we reduce the volume fraction of interacting sites present in the polymer chains can we prepare a true solution of the two polymers in a common solvent and, furthermore, produce a coherent film of the blend of the same composition by evaporation of the solvent?" In other words, by manipulating the volume fraction of interacting sites available, can we arrive at a compromise that results in a film forming miscible blend?

The solution behavior of P2VP mixtures with EMAA copolymers of varying composition in THF is summarized in Table I. Immediate turbidity is produced over the complete blend composition range when clear dilute THF solutions of P2VP are mixed together with EMAA[55] or EMAA[44] in the same solvent. A similar observation is made for EMAA[32] mixtures in compositions of greater than about 50 wt % P2VP. On the other hand, true, clear THF solutions are formed of EMAA[18]-P2VP mixtures over the entire composition range and for EMAA[32]-P2VP mixtures containing less than about 50 wt % P2VP. Coherent films can be readily cast from these blend solutions onto KBr windows for transmission infrared analysis.

In simple terms, the precipitation of polymer "complex" from a common solvent in which both polymers were initially soluble is a manifestation of the more favorable attraction of the two different polymers for one another than either polymer-solvent pair. Ultimately, of course, it is a balance between the free energy contributions involved. Introducing chemical units into the polymer chain that are not capable of forming relatively strong intermolecular interactions with complimentary units of the other polymer chain alters this balance. At some point, solution of the two polymers in the common solvent becomes more favorable than phase separation (precipitation). It is not our intent to systematically describe the FTIR results obtained on all the EMAA blends. In those cases that resulted in turbid solutions the mixtures can be separated by centrifugation into a precipitate and a supernatant liquor. We will not elaborate upon these FTIR results as the general conclusions are similar to those described previously for the PVP-P2VP complexes.<sup>20</sup> Rather, we wish to emphasize the results obtained by using conventional transmission FTIR spectroscopic studies of coherent film samples of polymer mixtures of known composition.

Figure 3 shows scale expanded FTIR spectra over the range of 1800-3800  $\text{cm}^{-1}$ . A film cast from a clear THF solution containing 65:35 wt % of EMAA[32]:P2VP was employed. Spectra were recorded as a function of temperature as the sample was heated to 140 °C (below the onset of anhydride formation<sup>3</sup>) and then cooled back down to room temperature. As one might expect, the characteristic infrared bands indicative of strong hydrogen bonding between the carboxylic acid and pyridine moieties are immediately apparent at 1950 and 2530  $\text{cm}^{-1}$ . This, of course, indicates that intermolecular interactions are occurring between the two polymers in the blend which, in turn, suggests a significant degree of mixing has taken

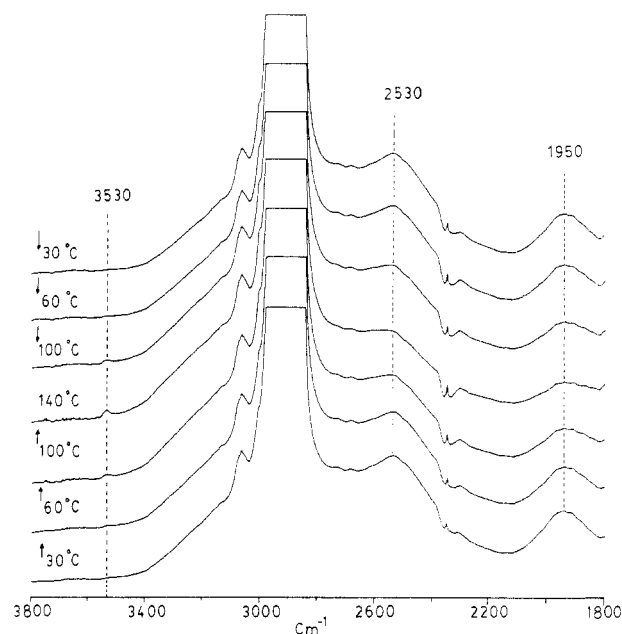


Figure 3. Scale expanded transmission infrared spectra in the 1800-3800  $\text{cm}^{-1}$  region obtained on a film of a 65:35 EMAA[32]-P2VP blend recorded as a function of temperature.

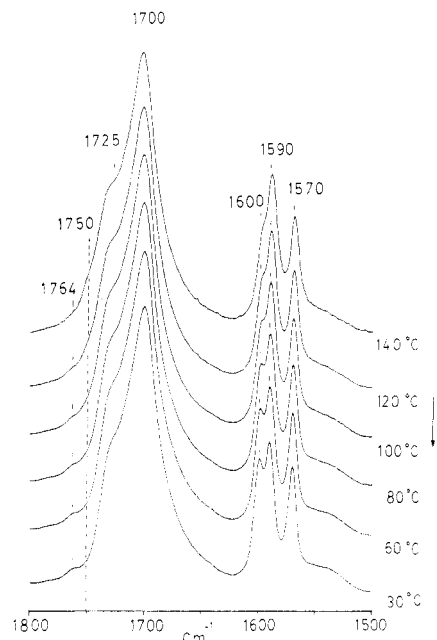


Figure 4. Scale expanded transmission infrared spectra in the 1500-1800  $\text{cm}^{-1}$  region obtained on a film of a 65:35 EMAA[32]-P2VP blend recorded as a function of decreasing temperature.

place. Infrared bands attributed to the carboxylic acid dimer (self-association of the EMAA copolymer) are still in evidence, albeit masked somewhat by the CH stretching modes. The effect of temperature, at least up to 140 °C, is not dramatic. This might be expected given the relative strength of the hydrogen bond involved and the limited temperature range covered. A measurable decrease in the intensity of the 1950  $\text{cm}^{-1}$  band is observed, however, which recovers when cooled to room temperature. The small band detected at 3530  $\text{cm}^{-1}$  in the 140 °C spectrum is consistent with the formation of a very small concentration of "free" acid groups.

Figure 4 shows the 1500-1800  $\text{cm}^{-1}$  region of the infrared spectrum of the same EMAA[32]-P2VP film sample. Only the cooling part of the cycle from 140 °C is shown as the spectra recorded during heating are essentially superim-

posable at identical temperatures. In the carbonyl stretching region of the spectrum, the  $1700\text{ cm}^{-1}$  band attributed to the intermolecular carboxylic acid dimer (self-association of EMAA[32]) dominates. The contribution at  $1725\text{ cm}^{-1}$  is assigned to the "free" carbonyl group liberated when the complex between the acid hydroxyl and the pyridine nitrogen group is formed. A knowledge of the absorptivity ratio of these two bands permits a quantitative measure of the fraction of the interacting species. In common with the O-H stretching region, the effect of temperature (up to  $140\text{ }^{\circ}\text{C}$ ) on the carbonyl stretching region is minimal. The slight absorbance detected at  $1750\text{ cm}^{-1}$  in the elevated temperature spectra is consistent with the presence of a trace of acid monomer.

A most interesting trio of infrared bands appearing at  $1570$ ,  $1590$ , and  $1600\text{ cm}^{-1}$  deserve special mention. As stated above, the bands at  $1570$  and  $1590\text{ cm}^{-1}$  are essentially ring modes of the pyridine group. Upon mixing P2VP with EMAA[32], a new band at  $1600\text{ cm}^{-1}$  is observed. This band is characteristic of the pyridine-carboxylic acid interaction<sup>23</sup> and results from a perturbation of the  $1590\text{ cm}^{-1}$  ring mode. Conversely, the  $1570\text{ cm}^{-1}$  band appears insensitive to the formation of the complex—a fact we will use to our advantage in our forthcoming quantitative measurements. In the room-temperature spectrum of the blend (see Figure 4) these three bands are well-resolved. As the temperature is raised, the intensity of the  $1600\text{ cm}^{-1}$  band appears to decrease but this is complicated by a concurrent shift to lower frequency. In any event, these two bands ( $1590$  and  $1600\text{ cm}^{-1}$ ) are sensitive to changes of the strength of the acid-pyridine interaction.

Having set the stage, we are now in a position to attempt the quantitative measurement of the number of specific interactions present in a methacrylic acid-pyridine polymer blend system as a function of composition. However, the EMAA[32]-P2VP system is not soluble in THF over the complete composition range (Table I), and there is the unfortunate complication of a significant amount of polyethylene type crystallinity present in the EMAA[18]-P2VP blends in the solid state at ambient temperatures (in effect, a "crystalline" compatible blend). Accordingly, for the remainder of this study we will concentrate on the transmission infrared spectral results obtained by using films prepared from the EMAA[32]-SP2VP[70] blend system. In essence, we have reduced the volume fraction of pyridine groups in the P2VP polymer by copolymerizing with inert styrene groups. It should be emphasized that a true solution of this polymer mixture can be prepared in THF. Thus, clear coherent films can be readily prepared by solvent casting at any desired blend composition.

Thermal analysis of these blends supports the contention that the EMAA[32]-SP2VP[70] is indeed miscible. Pure SP2VP[70] has a  $T_g$  of  $99\text{ }^{\circ}\text{C}$ . Thermograms of blends containing 20 and 40 wt % EMAA[32] yielded single distinctive  $T_g$ 's at  $63$  and  $38\text{ }^{\circ}\text{C}$ , respectively. At higher concentrations of EMAA[32] in the blend, partial crystallization occurs, the thermogram becomes more complex and it is not possible to unambiguously identify a  $T_g$ . However, at 80 wt % EMAA[32] we once again observe an apparent  $T_g$  at  $-2\text{ }^{\circ}\text{C}$  (resolved because the  $T_g$  of the blend is separated away from the transitions due to crystallinity). A plot of the experimental  $T_g$ 's as a function of the blend composition together with the best Fox-Flory curve fit to these results is shown in Figure 5.

Figure 6 shows *scale expanded* room-temperature FTIR spectra in the  $1620$ – $1800$  and  $1520$ – $1640\text{ cm}^{-1}$  ranges of

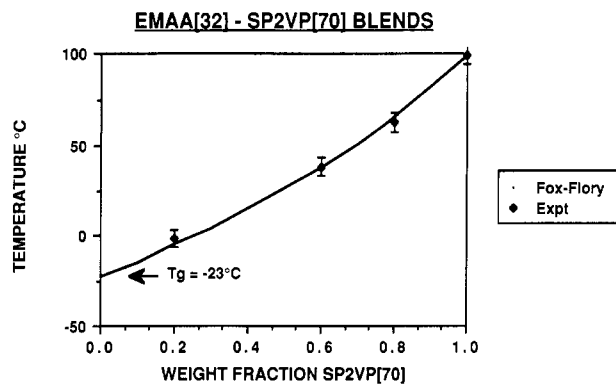


Figure 5. Graph of  $T_g$  versus EMAA[32]-SP2VP[70] blend composition. The solid line was calculated from the Fox-Flory relationship.

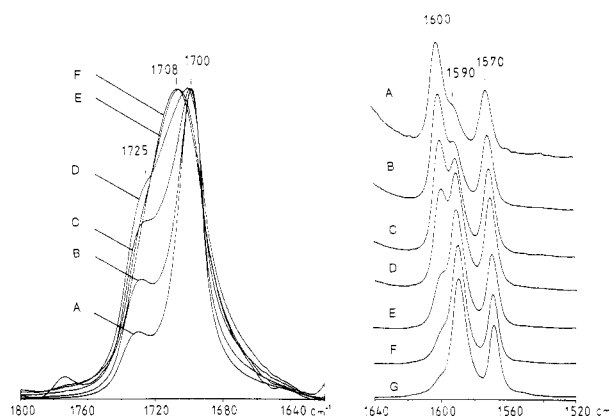


Figure 6. Scale expanded transmission infrared spectra recorded at room temperature in the  $1520$ – $1640$  and  $1640$ – $1800\text{ cm}^{-1}$  regions of EMAA[32]-SP2VP[70] blend samples: (A) 90:10, (B) 80:20, (C) 70:30, (D) 60:40, (E) 40:60, (F) 10:90, and (G) 0:100 wt % EMAA[32]:SP2VP[70].

EMAA[32] blends of varying composition with SP2VP[70]. The blends characteristic of strong hydrogen bonds at  $2530$  and  $1950\text{ cm}^{-1}$  are prominent in the spectra of these blends but are not shown since they closely resemble those displayed in Figure 3. Let us first turn our attention to the carbonyl stretching region of the spectrum (left hand side of Figure 6). Spectra are shown of blend films containing 90, 80, 70, 60, 40, and 20 wt % EMAA[32]. As the concentration of SP2VP[70] in the blend is increased up to about 50 wt %, the band attributed to the carboxylic acid-pyridine interaction, i.e., the "liberated" C=O group at approximately  $1725\text{ cm}^{-1}$ , increases at the expense of the carboxylic acid dimer ( $1700\text{ cm}^{-1}$ ). This is reminiscent of analogous results reported for the EMAA-PVME blend system<sup>8</sup> and is entirely consistent with a high degree of mixing of the two polymers at the molecular level. In marked contrast, however, the presence of excess pyridine groups (i.e. blend compositions rich in SP2VP[70]) leads to a single intermediate broad band centered at approximately  $1708\text{ cm}^{-1}$ . Separate contributions from carboxylic acid dimers and carboxylic acid-pyridine interactions are not now obvious. As we will see later, this is consistent with a rapidly decreasing concentration of carboxylic acid dimers in blend compositions of greater than 50 wt % SP2VP[70] and would not be easy to measure accurately even under ideal conditions. Additionally, it is most probable that in the presence of excess pyridine groups, the "liberated" carbonyl group attributed to the carboxylic acid-pyridine interaction is broadened and shifted to lower frequency through polar interactions. In any event, this unfortunate complication prevents us from using this re-

Table II  
Curve-Fitting Data from Infrared Spectra of EMAA[32]-SP2VP[70] Blends

EMAA[32] mol fractn	$\nu_1$ , cm <sup>-1</sup>	$W_{1/2}$ , cm <sup>-1</sup>	area $A_1$	$\nu_2$ , cm <sup>-1</sup>	$W_{1/2}$ , cm <sup>-1</sup>	area $A_2$	$\nu_3$ , cm <sup>-1</sup>	$W_{1/2}$ , cm <sup>-1</sup>	area $A_3$	fractn "free" py	fractal area of $A_3$
0.83	1600	10	64	1590	12	18	1571	8	28	0.22	0.25
0.69	1600	10	173	1589	10	63	1570	10	100	0.27	0.30
0.57	1599	11	179	1589	10	117	1570	9	120	0.40	0.29
0.46	1599	11	222	1589	10	231	1570	8	180	0.51	0.28
0.27	1599	9	224	1589	9	616	1569	7	300	0.73	0.26
0.12	1600	10	164	1589	9	988	1569	7	397	0.86	0.26

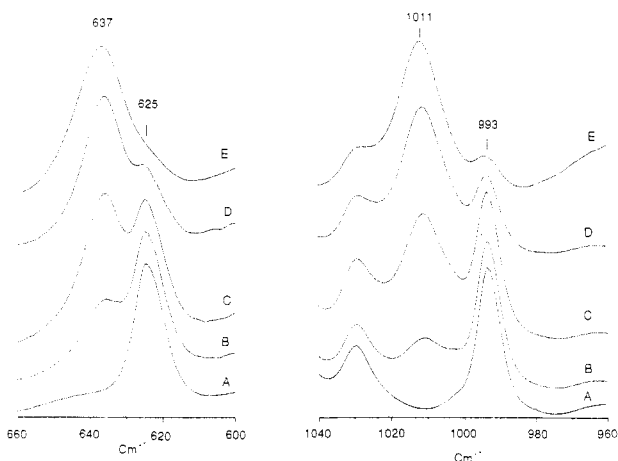


Figure 7. Scale expanded transmission infrared spectra recorded at room temperature in the 600–660 and 960–1040 cm<sup>-1</sup> regions of EMAA[32]-SP2VP[70] blend samples: (A) 0:100, (B) 20:80, (C) 40:60, (D) 60:40, and (E) 80:20 wt % EMAA[32]:SP2VP[70].

gion of the spectrum for simple quantitative analysis.

All is not lost, however. The 1600/1590 cm<sup>-1</sup> bands, attributed to pyridine groups that are and are not involved in intermolecular interactions with the carboxylic acid groups in the blends, are shown on the right-hand side of Figure 6. The styrene group also exhibits weak absorption in this region of the spectrum, but fortunately, as the spectrum of pure SP2VP[70] in this region shows (spectrum 6G), the interference is minimal. As the concentration of EMAA[32] is increased in the blend, there is a corresponding increase in the relative intensity of the 1600 cm<sup>-1</sup> band while that of the 1590 cm<sup>-1</sup> band decreases. Parallel changes are also observed for the pyridine ring modes at 1011/993 and 637/624 cm<sup>-1</sup>, shown in Figure 7. Although all three spectral regions appear to lend themselves to quantitative analysis, the former is particularly convenient because the baseline is well-defined and, more importantly, the 1570 cm<sup>-1</sup> band appears unaffected by the presence of the EMAA copolymer and may be used as an internal standard.

The spectra obtained were of excellent quality, and it was a straightforward task to draw a linear base line from 3800 to 500 cm<sup>-1</sup> through regions where there is little or no absorption. The three bands in the 1520 to 1640 cm<sup>-1</sup> region are relatively narrow and essentially Lorentzian in character. Accordingly, a least-squares fit of three Lorentzian curves was performed, and the results are given in Table II. The fraction of "free" pyridine groups,  $f_F^N$  (i.e. those SP2VP[70] pyridine groups not hydrogen bonded to EMAA[32] carboxylic acid groups), is defined as

$$f_F^N = \frac{A_{1570}}{A_{1570} + \frac{a_{1600}}{a_{1590}} A_{1600}} \quad (1)$$

where  $A$  and  $a$  are the intensities (areas) and absorption coefficients, respectively, for the bands identified. There is reason to be confident that little error will be introduced

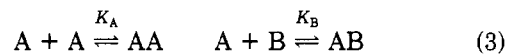
if an absorptivity ratio of unity is assumed. The 1570 cm<sup>-1</sup> pyridine ring mode appears unaffected by the presence of carboxylic acid groups<sup>23</sup> and may be considered an internal standard. Consequently, major differences in the magnitude of the absorption coefficients of the 1590 and 1600 cm<sup>-1</sup> bands should yield a systematic change in the fractional area of the 1570 cm<sup>-1</sup> band with blend composition. This is not observed and the fractional area of the 1570 cm<sup>-1</sup> band relative to the total area of all three bands ( $A_{1570} + A_{1590} + A_{1600}$ ) remains essentially constant (within 10%) at 0.28 (see Table II). Equation 1 thus reduces to

$$f_F^N = \frac{A_{1570}}{A_{1570} + A_{1600}} \quad (2)$$

The estimated fraction of "free" pyridine groups in the blends of varying molar composition are also included in Table II. A range of approximately 14–78% of the pyridine groups are involved in intermolecular interactions with the EMAA carboxylic acid groups as the molar composition of EMAA[32] in the blend increases from 12 to 83%.

### Theoretical Considerations—Competing Equilibria

The blends of the EMAA copolymers with P2VP and SP2VP[70] discussed above may be again described in terms of two competing equilibria in a manner similar to other polymer blend systems described recently.<sup>1-3</sup> Equilibrium constants,  $K_A$  and  $K_B$ , are used to express the self-association of EMAA[32] and the association of EMAA[32] with SP2VP[70], respectively, as depicted below.



$$K_A = \xi_{AA}/\xi_A^2 \quad K_B = \xi_{AB}/\xi_A\xi_B \quad (4)$$

Where  $\xi_A$ ,  $\xi_B$ ,  $\xi_{AA}$ , and  $\xi_{AB}$  are the mole fractions of A, B, AA, and AB units in the mixture at equilibrium. Following Flory<sup>24</sup> we have noted that in systems where chains of hydrogen-bonded groups are formed the equilibrium constants are more correctly defined in terms of molar concentrations. As Sarolea-Mathot<sup>25</sup> has shown, however, the errors involved using mole fractions are not large in simple monomer-dimer systems. In order to demonstrate the dependence of complex formation on composition, we will use the simple mole fraction approach here and present a more rigorous description of the thermodynamics of these systems in a separate publication.

We have shown previously<sup>3</sup> that  $X_A$ , the initial mole fraction of A units in the blend, may be expressed as

$$X_A = \frac{(1 + K_B)\xi_A + 2K_A\xi_A^2 + K_A K_B \xi_A^3}{1 + 2K_B\xi_A + (K_A - K_B)\xi_A^2} \quad (5)$$

Since we have independently determined<sup>3</sup> the value of  $K_A$  at room temperature for the EMAA copolymers at  $2 \times 10^4$ , this equation may be solved numerically by assum-

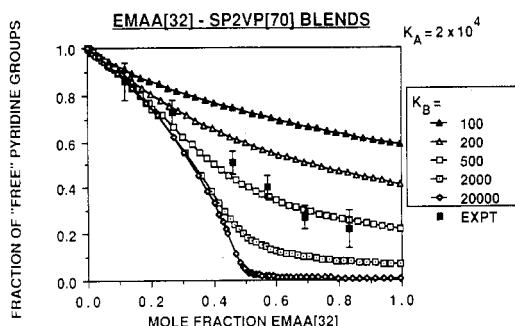


**Figure 8.** Plot of the fraction of "free" pyridine groups versus the mole fraction of EMAA[32] in blends with SP2VP[70] at room temperature. The solid lines are calculated by using the values of  $K_B$  indicated—see text.

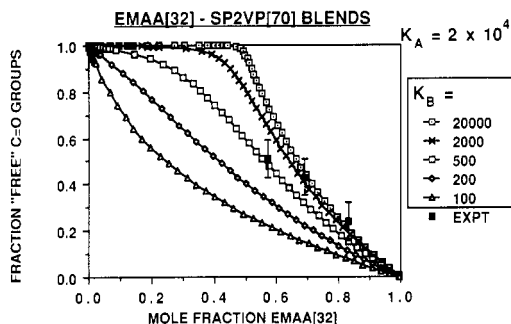


**Figure 9.** Plot of the fraction of "free" carbonyl groups versus the mole fraction of EMAA[32] in blends with SP2VP[70] at room temperature. The solid lines are calculated by using the values of  $K_B$  indicated—see text.

ing values of  $K_B$ . Accordingly, values of  $X_A$  are calculated over the range from zero to unity by using appropriate values of  $\xi_A$ . The parameters  $\xi_{AA}$ ,  $\xi_B$ , and  $\xi_{AB}$  are then readily calculated. The theoretical fraction of "free" pyridine groups,  $f_F^N$ , is defined as  $\xi_B / (\xi_B + \xi_{AB})$ , and this may be compared directly to the experimental data, as it is equivalent to what we have measured in the infrared spectra. A comparison of the experimental blend data (Table II) with theoretical curves of the fraction of "free" pyridine groups versus mole fraction of EMAA using appropriate values of  $K_B$  is displayed graphically in Figure 8. Theoretical curves were determined for  $K_B$  values of  $2 \times 10^4$ ,  $2 \times 10^3$ , 500, 200, and 100. The experimental data for the EMAA[32]-SP2VP[70] blends parallels the theoretical curve obtained for  $K_B = 500$ . Thus the magnitude of  $K_B$  in this case is some 40 times less than that of  $K_A$ . (Again we emphasize that the equilibrium constant is related to the enthalpy and entropy of hydrogen bond formation via the well-known relationship,  $\ln K = -\Delta H/RT + \Delta S/R$ . Accordingly, in these terms,  $\ln K_A$  and  $\ln K_B$  (9.9 and 6.2, respectively) differ only by a factor of about 1.6.)

In our previous paper<sup>3</sup> concerning EMAA blends with PVME and EPO we were able to quantitatively measure the fraction of "free" C=O groups over the entire composition range. (Recall, in this case the "free" or liberated C=O group corresponds to an interaction involving the carboxylic acid and pyridine groups). As mentioned above, it was not possible to measure the fraction of "free" C=O groups in the EMAA[32]-SP2VP[70] blends over the whole composition range. Nevertheless, we can still calculate a theoretical fraction of "free" carbonyl groups,  $f_F^{CO}$ , defined as  $\xi_{AB} / (\xi_{AB} + 2\xi_{AA})$ , using the same values of  $K_B$  as above. The results are shown graphically in Figure 9. Three experimental values of the fraction of "free" C=O groups obtained from the spectra of the EMAA[32] rich blends are included. These were determined by using an

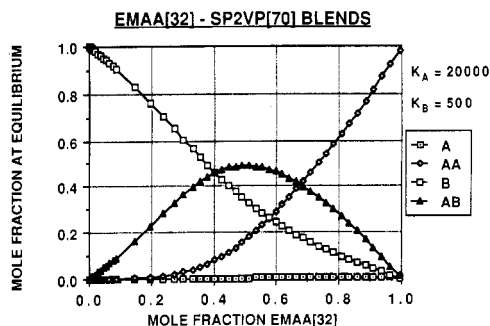


**Figure 10.** Calculated distributions of the mole fraction of A, AA, B, and AB species versus the mole fraction of EMAA[32] in blends with SP2VP[70] at room temperature assuming  $K_A$  and  $K_B$  values of  $2 \times 10^4$  and  $5 \times 10^2$ , respectively.

identical method to that described in our previous paper.<sup>3</sup> The two infrared bands, in these specific cases, are reasonably well-separated, but we frankly do not have much confidence in these data because of the inherent spectral complications mentioned above. Nevertheless, it is pleasing to see that the data do seem to be following a  $K_B$  value of approximately 500—the same as that seen for the "free" pyridine data (see Figure 8).

Having reasonable estimates of both  $K_A$  ( $2 \times 10^4$ ) and  $K_B$  ( $5 \times 10^2$ ), we can now calculate the mole fraction of the species A (acid monomer), AA (acid dimer), B (uncomplexed pyridine), and AB (acid-pyridine complex) as a function of blend composition. This is shown in Figure 10. Not surprisingly, the concentration of acid monomers is very small throughout the whole composition range. With increasing concentration of EMAA[32] in the blend, the mole fraction of acid dimers increases while that of the uncomplexed pyridine groups decreases. At the same time, the mole fraction of acid-pyridine complexes rises to a maximum and then decreases and has the form of a bell-shaped curve. We were particularly interested to see that at blend compositions of less than 40 mol % EMAA[32] (equivalent to approximately 50 wt %) the concentration of acid dimers and monomers becomes insignificant. AB species (acid-pyridine complexes) are present in a sea of B species (uncomplexed pyridine). It is at this point where we see no obvious contribution from the acid dimer in the infrared spectrum at  $1700 \text{ cm}^{-1}$  but do observe a broadening and shifting of the carbonyl band attributed to the acid-pyridine complex.

Finally, it is informative to compare the results obtained on the blends of the copolymer EMAA[32] with the two different polymers, PVME and SP2VP[70], at room temperature. The equilibrium constants,  $K_B$ , describing the association of the carboxylic acid group with either the ether oxygen of PVME<sup>3</sup> or the pyridine nitrogen group of SP2VP[70] differ significantly (100 versus 500, respectively). To some extent, this reflects the increased strength of the hydrogen bond in the latter case. However, it is important to recognize that even though the strength of the interaction between the EMAA carboxylic acid and SP2VP pyridine groups exceeds that of the carboxylic dimer (self-association), the magnitude of the carboxylic acid dimer equilibrium constant is greater—there is an entropic contribution to the hydrogen bond formation that cannot be ignored.

**Acknowledgment.** The financial support of the National Science Foundation, Polymers Program, and the donors of the Petroleum Research Fund, administered by the American Chemical Society, is greatly appreciated.

**Registry No.** EMAA, 25053-53-6; P2VP, 25014-15-7; (2VP)(S) (copolymer), 24980-54-9.



## References and Notes

- (1) Coleman, M. M.; Skrovanek, D. J.; Hu, J.; Painter, P. C. *Macromolecules* **1988**, *21*, 59.
- (2) Painter, P. C.; Park, Y.; Coleman, M. M. *Macromolecules* **1988**, *21*, 66.
- (3) Lee, J. Y.; Painter, P. C.; Coleman, M. M. *Macromolecules*, accepted for publication.
- (4) Moore, T. S.; Winmill, T. F. *J. Am. Chem. Soc.* **1979**, *101*, 1635.
- (5) Vinogradov, S. N.; Linnell, R. H. *Hydrogen Bonding*; Van Nostrand: New York, 1971.
- (6) Pimentel, G. C.; McClellan, A. L. *The Hydrogen Bond*, W. H. Freeman: San Francisco and London, 1960.
- (7) Pimentel, G. C.; McClellan, A. L. *Annu. Rev. Phys. Chem.* **1971**, *22*, 347.
- (8) Novak, A. *Struct. Bonding (Berlin)* **1974**, *18*, 177.
- (9) Schuster, P.; Zundel, G.; Sandorfy, C. *The Hydrogen Bond. Recent Developments in Theory and Experiments*; North Holland: New York, 1976; Vols. I-III.
- (10) Skrovanek, D. J.; Howe, S. E.; Painter, P. C.; Coleman, M. M. *Macromolecules* **1985**, *18*, 1676.
- (11) Skrovanek, D. J.; Painter, P. C.; Coleman, M. M. *Macromolecules* **1986**, *19*, 699.
- (12) Coleman, M. M.; Skrovanek, D. J.; Painter, P. C. *Makromol. Chem., Macromol. Symp.* **1986**, *5*, 21.
- (13) Coleman, M. M.; Lee, K. H.; Skrovanek, D. J.; Painter, P. C. *Macromolecules* **1986**, *19*, 2149.
- (14) Hadzi, D. *Chimia* **1972**, *26*, 7.
- (15) Hadzi, D. *Pure Appl. Chem.* **1965**, *11*, 435.
- (16) Odinov, S. E.; Mashkovsky, A. A.; Glazunov, V. P.; Logansen, A. V.; Rassadin, B. V. *Spectrochim. Acta, Part A* **1976**, *32a*, 1355.
- (17) Speakman, J. C. *Struct. Bonding (Berlin)* **1972**, *12*, 141.
- (18) Lippencott, E. R.; Schroeder, R. J. *J. Chem. Phys.* **1955**, *23*, 1099.
- (19) Lippencott, E. R.; Schroeder, R. J. *J. Phys. Chem.* **1957**, *61*, 921.
- (20) Lee, J. Y.; Moskala, E. J.; Painter, P. C.; Coleman, M. M. *Appl. Spectrosc.* **1986**, *40*, 991.
- (21) Hadzi, D.; Bratos, S. In *The Hydrogen Bond*; Schuster, P., Zundel, G., Sandorfy, C., Eds.; North Holland: New York, 1976; Vol. II, Chapter 12.
- (22) Fuller, M. P.; Griffiths, P. R. *Anal. Chem.* **1978**, *50*, 1906.
- (23) Takahashi, H.; Mamola, K.; Pyler, E. K. *J. Mol. Spectrosc.* **1966**, *21*, 217.
- (24) Flory, P. J. *J. Chem. Phys.* **1944**, *12*, 425.
- (25) Sarolea-Mathot, L. *Trans. Faraday Soc.* **1953**, *49*, 8.

## Structural Analysis of the Alternating Copolymer Poly(chloroacrylonitrile-*alt*-cyclohexadiene)

V. Panchalingam and John R. Reynolds\*

*Department of Chemistry, The University of Texas at Arlington, Arlington, Texas 76019.  
Received July 8, 1987*

**ABSTRACT:** 2-Chloroacrylonitrile and 1,3-cyclohexadiene have been copolymerized by using radical and coordination initiators. Elimination reactions were carried out in the brominated and the virgin copolymer using KF and a phase-transfer catalyst in order to prepare derivatives which facilitated in the characterization of the copolymer. <sup>13</sup>C NMR and attached proton test (APT) indicate that the HCl elimination from the virgin copolymer leads to the formation of a highly substituted olefin. FT-IR analyses of the copolymer and its derivatives suggest the formation of essentially 1,4-linkages across the cyclohexene unit. The copolymer microstructure has been characterized by <sup>1</sup>H NMR, two-dimensional proton *J*-correlated (COSY), <sup>13</sup>C NMR, DEPT, and two-dimensional <sup>1</sup>H-<sup>13</sup>C chemical shift correlated (CSCM) spectroscopic techniques. These studies indicate the presence of 1,4-linkages, while simultaneously suggesting the absence of a significant amount of 1,2-linkages in the copolymer.

### Introduction

Regular alternating copolymers are commonly synthesized from monomer pairs that form intermediate donor-acceptor complexes.<sup>1-5</sup> These systems include the diene-dienophile type in which the charge-transfer (CT) complex can also undergo competitive Diels-Alder cycloaddition reactions. Both cyclic and acyclic dienes, such as 1,3-pentadienes, 1,3-cyclohexadienes, furans, isoprene, butadiene, and piperylene, serve as electron donors in conjunction with electron acceptors, which include maleic anhydride, and polar vinyl monomers, such as acrylonitrile, 2-chloroacrylonitrile, and methyl 2-chloroacrylate.<sup>3-7</sup>

Polymerization of these CT complexes can occur spontaneously or can be initiated by numerous species with a substantial increase in polymerization rate. Typical initiators include free radical systems (AIBN, benzoyl peroxide), Lewis acids (ZnCl<sub>2</sub>, AlCl<sub>3</sub>), and metal salts (silver triflate).

Among these systems, the use of 1,3-cyclohexadiene (CHD) as the donor monomer is intriguing in that the copolymers formed may be used as a substrate for subsequent elimination or addition reactions. The ability to locate cyclohexene rings along a polymer chain may serve as a method of incorporating isolated phenyl rings in the polymer after aromatization. In this manner, polyphenylenes have been synthesized under severe conditions

from unsubstituted cyclohexadienes<sup>8</sup> while more recently the use of the acetate derivative of 5,6-dihydroxy-1,3-cyclohexadiene,<sup>9,10</sup> has yielded high molecular weight polyphenylenes under milder conditions.

The mechanism of polymerization of 1,3-CHD can proceed via either 1,2- or 1,4-additions across the ring. For example in the case of diester substituted CHD's, the relative content of 1,2 versus 1,4 structures has been found to be a function of ester type.<sup>10</sup> In the case of the alternating copolymerization of 1,3-CHD and polar vinyl monomers the mechanism of polymerization through the CHD ring has not been fully elucidated.<sup>11</sup>

In this paper, we describe the structure of the copolymer poly(2-chloroacrylonitrile-*co*-1,3-cyclohexadiene), hereafter labeled poly(CAN/CHD), utilizing TGA, FT-IR, <sup>13</sup>C and <sup>1</sup>H NMR, 2D <sup>13</sup>C<sup>1</sup>H correlated (CSCM), 2D COSY, <sup>13</sup>C-distortionless enhancement by polarization transfer (DEPT), and attached proton test (APT) spectroscopy. Two-dimensional NMR techniques have previously been used in characterizing copolymer microstructure.<sup>12</sup> Derivatives of this copolymer, synthesized via either addition (bromination) or elimination reactions, have been used in structure confirmation.

### Experimental Section

**Materials and Methods.** 1,3-CHD (98% Aldrich Chemical) was distilled over CaH<sub>2</sub>. 2-Chloroacrylonitrile (99% Aldrich